D18

Operando Raman Imaging of Wear and Deformation Processes

TII/早大（正）*ベルツ　モルテン、（正）柳沢　雅広、（非）本間　敬之

Morten Bertz*, **, Masahiro Yanagisawa**, Takayuki Homma**

*Tokyo Instruments, **Waseda University

1. Introduction

Operando observations, i.e. investigating a system as closely as possible to actual operating conditions, are key to obtain a deeper understanding of material properties Here, we discuss results obtained using a multi-messenger approach that combines Raman imaging, bright-field microscopy, and mechanical measurements to reveal spatially resolved chemical and physical changes of materials subjected wear or deformation.

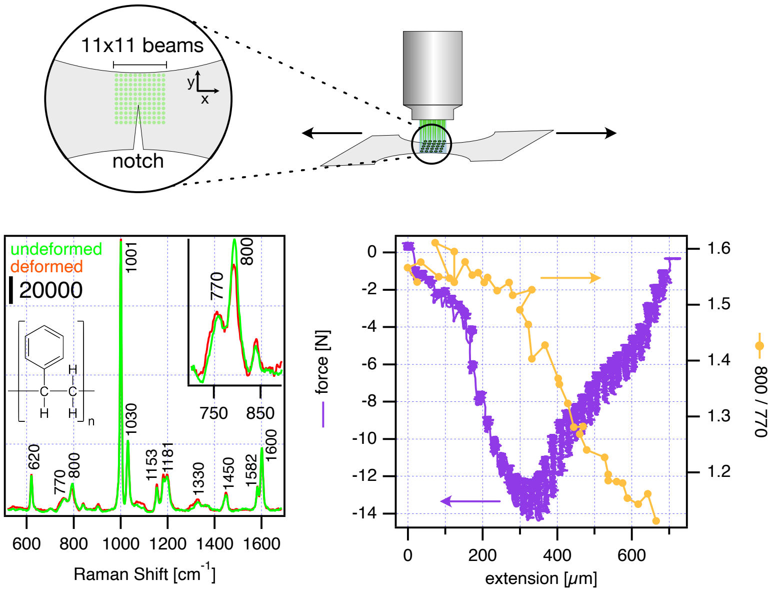

Fig. 1 (Top) Schematic of the experiment. A notched polymer sample is probed by multipoint Raman imaging while undergoing uniaxial deformation. (Bottom) Sample data for a polystyrene film.

2. Methods

Raman imaging was performed using a Phalanx Raman microscope (Tokyo Instruments) equipped with a 532 nm laser and a 5x objective lens. Bright field images were simultaneously recorded through the same lens using narrow-band 450 nm LED illumination. For deformation experiments, the incident laser light was polarized parallel to the direction of deformation (x direction in Fig. 1). In a typical deformation experiment, an area of 1.6×1.6 mm was imaged at 50 μm resolution during stepwise stretching by scanning a beam array of 11×11 beams across the sample. For wear experiments, an imaging area of 550 μm×550 μm (121 spectra in a single exposure) was monitored at 1.8 s intervals during rotation (60 rpm).

3. Results

Deformation experiments were performed by imaging the necking region during stepwise elongation of thin polymer films (Fig. 1, top). Using a polystyrene film as an example, Fig. 1 (bottom left) shows changes in the characteristic Raman spectrum before and after deformation. In particular, the ratio between the peaks at 770 cm^{-1} and 800 cm^{-1}, which reflect long trans and mixed trans / gauche regions of the polymer backbone [1], changes upon deformation. These two bands are commonly used to monitor polystyrene crystallinity [2]. The relative increase in the peak at 770 cm^{-1} indicates an orientation of the crystalline units along the pulling direction as stress is applied to the sample. This conformational change coincides with the yield point of the material (Fig. 1, bottom right). High-resolution hyperspectral Raman imaging reveals the spatial distribution of these changes (Fig. 2). While crystallinity was homogenous across the undeformed sample (Fig. 2. top), microstructural changes reported by the ratio of the conformationally sensitive 770 cm^{-1} / 800 cm^{-1} band pair became apparent once the sample was stretched to (Fig. 2 center) or beyond the yield point (Fig. 2 bottom). The microstructural changes occur in

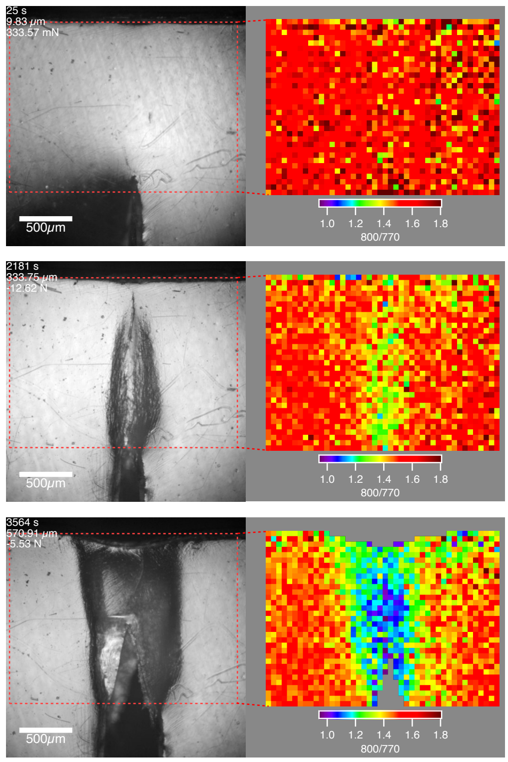

Fig. 2 Bright-field (left) and Raman images (right) of a polystyrene film at different stages of deformation.

regions of the sample with visible changes in appearance, i.e. necking. In addition to changes in crystallinity and orientatation, Raman spectra also reveal load sharing and local ordering via peak position and line widths. Furthermore, image analysis of the simultaneously acquired bright-field images allows the computation of local strain of the notched sample to directly correlate structural changes with local mechanical parameters.

Wear experiements were conducted by monitoring the sample surface during rotation through a transparent, hemispherical sliding element using simultaneous Raman and brightfield imaging (Fig. 3, top). Our multi-point Raman microscope permits the acquitsion of a hyperspectral Raman image consisting of 11×11 spectra (corresponding to a 550 μm×550 μm observation area) in a single exposure. Snapshot obtained during the wear process of a sapphire lens sliding against a crystalline silicon surface and are shown at the bottom of Fig. 3. While the observation area initially contains only crystalline sillicon (indicated by the 520 cm^{-1} peak, red), a black wear track starts forming after around 35 revolutions, which consists of amorphous silicon (500 cm^{-1} peak, blue) [3]. The wear track continues to widen as rotation progresses and eventually occupies the entire field of view but Raman imaging shows that the distribution of accumulated amorphous silicon debris is not homogeneous and islands of crystalline silicon can be discerned. In addition to local chemical information, Raman images also reveal the local temperature of the sample undergoing frictional heating.

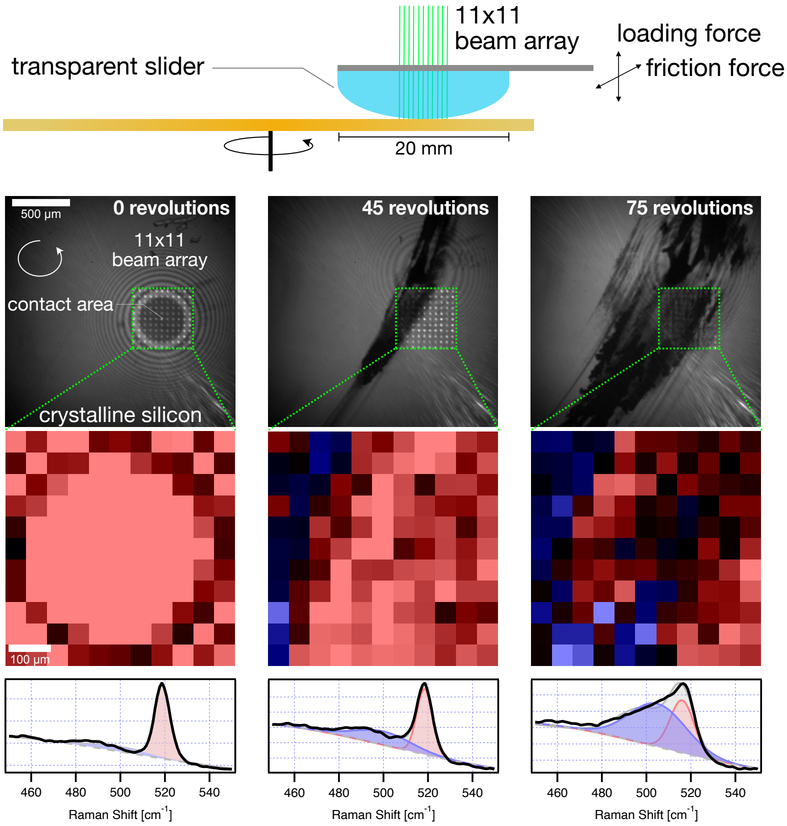

Fig. 3 (Top) Schematic of the experiment: Imaging of surface wear through a transparent sliding element. (Bottom) snapshots of a silicon surface during the wear process using simultaneous bright-field and Raman imaging. (crystalline silicon: red, amorphous silicon: blue)

4. Conclusion

Our results demonstrate that operando Raman imaging can provide a wealth of insights into the structural-mechanical relationships of deformation and wear processes. Our multi-messenger approach yields spatially resolved chemical information along with sample morphology and mechanical parameters. We anticipate that multimodal operando Raman imaging will contribute to the understanding of a wide range of other tribological phenomena

Acknowledgements

This work was supported by the JST A-STEP program「プラズモンセンサを用いた超高感度表面・界面分析用表面増強ラマン顕微鏡の開発」(JPMJTR202K).

References

[1] Kellar, E. J. C., Galiotis, C., & Andrews, E. H. (1996). Raman Vibrational Studies of Syndiotactic Polystyrene. 1. Assignments in a Conformational/Crystallinity Sensitive Spectral Region. *Macromolecules*, *29*(10), 3515-3520. https://doi.org/10.1021/ma950772t

[2] Zhang, S. L., Pezzuti, J. A., Morris, M. D., Appadwedula, A., Hsiung, C.-M., Leugers, M. A., & Bank, D. (1998). Hyperspectral Raman Line Imaging of Syndiotactic Polystyrene Crystallinity. *Applied Spectroscopy*, *52*(10), 1264-1268. https://doi.org/10.1366/0003702981942753

[3] Schaeberle, M. D., Tuschel, D. D., & Treado, P. J. (2001). Raman Chemical Imaging of Microcrystallinity in Silicon Semiconductor Devices. Applied Spectroscopy, 55(3), 257-266. https://doi.org/10.1366/0003702011951867